GUIDED WAVE SCATTERING BY A CYLINDRICAL FLAW

Liviu Singher, Yitzhak Segal
Department of Quality Assurance and Reliability

Joseph Shamir
Department of Electrical Engineering
Technion - Israel Institute of Technology
Haifa 32000, Israel

INTRODUCTION

The evaluation of adhesive bonds involves the detection of the continuity of the adhesive and also its effective elastic properties. There are several advantages in employing guided waves for interface testing: the intensification of the measured effects along the path of the wave propagation, the possibility of testing very thin adhesive layers, only one dimensional scanning is necessary and they are less sensitive to the variations in the properties of the adherends relative to the method of ordinary bulk ultrasonic wave. The impinging guided ultrasonic wave is scattered by flaws embedded inside the adhesive layer. By examining the characteristics of the scattered field from the flaw, it is possible to extract useful information about the flaw location and its dimension. This study presents a computational solution to the ultrasonic scattering of guided waves, in an adhesive layer, by a cylindrical flaw. The scattering field contains information about the integrity of the adhesive layer. We consider the case of an adherend-adhesive-adherend sandwich. The adhesion strength is assumed to be good and uniform.

The problem of acoustic scattering from bodies of arbitrary shape is long standing. The extensive body of work goes as far back as the 1950s [1]. The problem has been treated by several numerical methods, usually formulated as a volumetric integral equation in which the pressure inside the body is the unknown to be determined. Accordingly to the proposed method, we set up two simulated equivalent situations, inside and outside the flaw cylinder, using two sets of fictitious spatially periodic isotropic filamentary ultrasonic sources of yet-to-be-determined constant complex amplitudes, as expansion functions for the unknown fields. So constructed, the simulated fields are now required to obey the continuity condition for the components of the displacement and stress at a suitable number of points on the cylinder surface. The result is a matrix equation in which the various matrices are interpreted in terms of generalized network parameters. The matrix equation is then solved for the unknown filamentary sources, which in turn are used to determine the

Review of Progress in Quantitative Nondestructive Evaluation, Vol. 16
Edited by D.O. Thompson and D.E. Chimenti, Plenum Press, New York, 1997

field inside and/or outside the cylinder. The procedure is very convenient to execute. This novel procedure is used to investigate the scattering of the guided waveforms incident on a flaw in the adhesive layer.

ANALYSIS OF DEFECTS WITHIN THE ADHESIVE LAYER

The discussion relates to the analysis of the influence of a flaw located in the adhesive layer. Such a flaw could deteriorate the bond strength to a cohesive failure. The dominant type of defect in the production of laminate structures is an air bubble. The obvious choice of geometry for a single scatterer is either the cylindrical or the spherical; the former was chosen in order to make the analysis susceptible to the case of two dimensional waveguide.

Extensive analysis of the guided wave transduction can be found in Ref. [2]. We shall present the pertaining formulation of a guided wave in a three layer laminant. The wave equation of an elastic, homogeneous, isotropic media, in terms of the displacement $u(y,z,t)$, is given in Ref. [3]. The solution is a combination of a longitudinal wave, $u = \nabla\phi$, and a transversal wave, $u = \nabla \times \psi$. We assume that the solutions are time harmonic of the form $\exp(-i\omega t)$ with z dependence of the form $\exp(ikz)$. The displacements and stresses are expressed in each region:

$|y| < h$

$$
\begin{aligned}
u_z &= \{ik[A_0\cosh(\alpha_0 y) + B_0\sinh(\alpha_0 y)] - \beta_0[C_0\sinh(\beta_0 y) + D_0\cosh(\beta_0 y)]\}\cdot\exp(ikz)\\
u_y &= \{\alpha_0[A_0\sinh(\alpha_0 y) + B_0\cosh(\alpha_0 y)] + ik[C_0\cosh(\beta_0 y) + D_0\sinh(\beta_0 y)]\}\cdot\exp(ikz)\\
t_{yy} &= \{\mu_0(k^2+\beta_0^2)[A_0\cosh(\alpha_0 y) + B_0\sinh(\alpha_0 y)] + 2\mu_0 ik\beta_0[C_0\sinh(\beta_0 y) + \\
&\quad + D_0\cosh(\beta_0 y)]\}\cdot\exp(ikz) \qquad (1)\\
t_{zy} &= \{2\mu_0 ik\alpha_0[A_0\sinh(\alpha_0 y) + B_0\cosh(\alpha_0 y)] - \mu_0(k^2+\beta_0^2)[C_0\cosh(\beta_0 y) + \\
&\quad + D_0\sinh(\beta_0 y)]\}\cdot\exp(ikz)
\end{aligned}
$$

$y > h$

$$
\begin{aligned}
u_z &= \{ikA_1\exp[-\alpha_1(y-h)] + \beta_1 B_1\exp[(-\beta_1(y-h)]\}\cdot\exp(ikz) \qquad (2)\\
u_y &= \{-\alpha_1 A_1\exp[-\alpha_1(y-h)] + ikB_1\exp[(-\beta_1(y-h)]\}\cdot\exp(ikz)\\
t_{yy} &= \{\mu_1(k^2+\beta_1^2)[A_1\exp[-\alpha_1(y-h)] - 2\mu_1 ik\beta_1 B_1\exp[-\beta_1(y-h)]\}\cdot\exp(ikz)\\
t_{zy} &= \{-2\mu_1 ik\alpha_1 A_1\exp[-\alpha_1(y-h)] - \mu_1(k^2+\beta_1^2)B_1\exp[-\beta_1(y-h)]\}\cdot\exp(ikz)
\end{aligned}
$$

$y < -h$

$$
\begin{aligned}
u_z &= \{ikA_2\exp[\alpha_2(y+h)] + \beta_2 B_2\exp[(\beta_2(y+h)]\}\cdot\exp(ikz) \qquad (3)\\
u_y &= \{-\alpha_2 A_2\exp[\alpha_2(y+h)] + ikB_2\exp[(\beta_2(y+h)]\}\cdot\exp(ikz)\\
t_{yy} &= \{\mu_2(k^2+\beta_2^2)[A_2\exp[\alpha_2(y+h)] - 2\mu_2 ik\beta_2 B_2\exp[\beta_2(y+h)]\}\cdot\exp(ikz)\\
t_{zy} &= \{-2\mu_2 ik\alpha_2 A_2\exp[\alpha_2(y+h)] - \mu_2(k^2+\beta_2^2)B_2\exp[\beta_2(y+h)]\}\cdot\exp(ikz)
\end{aligned}
$$

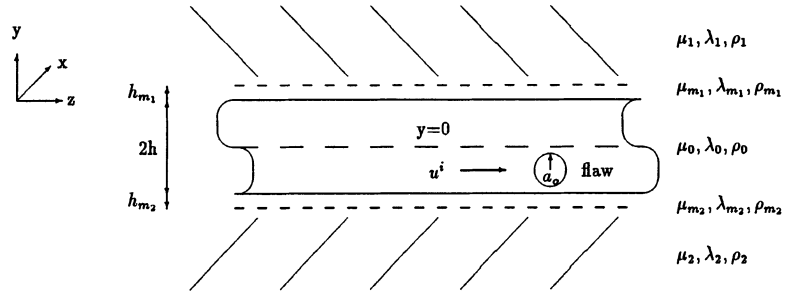

Figure 1: Geometry of the guiding system in an adhesive layer of thickness $2h$.

where V_l is the longitudinal wave velocity and V_t is the shear wave velocity in bulk medium, $\alpha^2 = k^2 - k_l^2$, $\beta^2 = k^2 - k_t^2$. k_l and k_t are the bulk propagation constants given by ω/V_l and ω/V_l respectively.

Although the method can be applied on an object of any arbitrary shape with smooth surface, this work deals with gas cavities in two dimension. Consider the scattering of a single frequency radiation of a true guided wave incident on an infinite cylindrical air bubble embedded in an adhesive layer, whose axis is taken to be parallel with the x axis of a rectangular coordinate system. A cross section of the cylinder embedded in the adhesive layer, together with a relevant coordinate system is shown in Fig. 1. The wave is propagating along the z direction through a three-layer structure, where the middle layer represents the adhesive layer, denoted by the index 0. The region surrounding the cylinder is the adhesive material. The bubble region is composed of air, located in the adhesive layer and excited by the incident guided wave. The cavity radius a_0 is determined to be smaller than the thickness h of the adhesive layer such that repeated interference of the scattered acoustic field from the adherend-adhesive interface, can be neglected. The extension of the following formulation to the multibody case is straightforward and will not be detailed here. For future convenience, we refer to the region external to the bubble but still well enclosed in the adhesive layer, as region I, to the bubble region as II and to the bubble surface bounding between these regions as S. Let the cylinder be immersed in an incident guided wave given by Eqs. (1)-(3). Our objective is to determine properties of the acoustic field scattered by the bubble. The suggested approach is to set up two simulated sets of line sources of yet unknown complex amplitudes which radiate the scattered and transmitted acoustic fields. These filaments are x-directed, infinite in extent and of wire type shape. One set of fictitious filaments is placed inside the flaw on a closed surface with radius a_1. These fictitious filaments simulate the scattered field outside the flaw, as shown in Fig. 2a. They radiate with constant amplitudes $\{A_i\}^I$, $i = 1, 2, \cdots, N^I$ where N^I is the number of the filaments. Since the acoustic scattered field is generated within the adhesive layer, the filament sources are simulated to radiate in an unbounded space, this space possessing the properties of the bulk adhesive material. The total field exterior to S is the sum of the incident field (u^i, t^i) due to the impressed incident field and the field (u^s, t^s) scattered from the body. Similarly, the transmitted field in the flaw, (u^t, t^t), is simulated by the second set of filaments as illustrated in Fig. 2b. These sources are treated as radiating in an

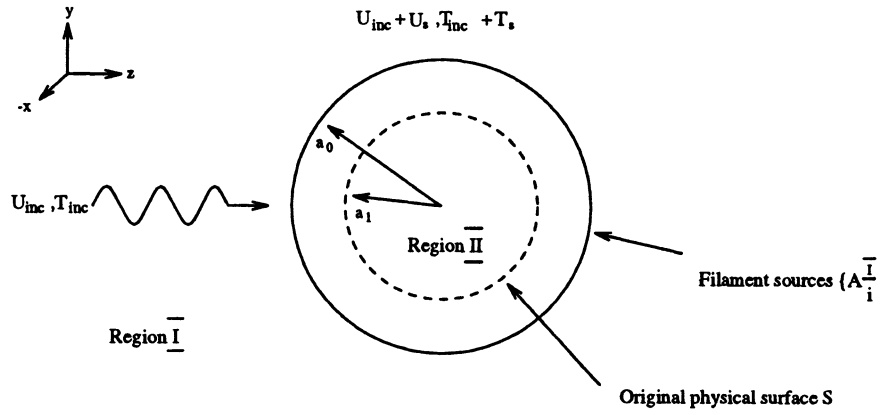

(a) Simulating the wave outside the object (scattered), region I

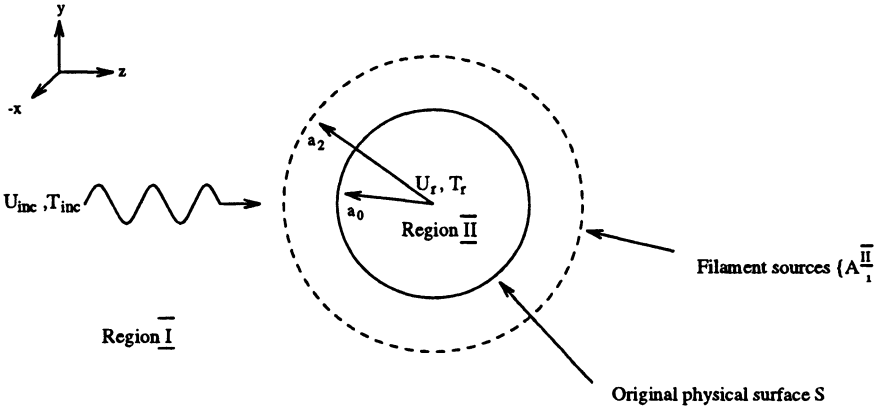

Figure 2: (b) Simulating the wave inside the object (refracted), region II

unbound space filled with homogeneous material identical to that composing the flaw. They are located on a closed surface enclosing S with radius a_2. These filaments radiate with constant amplitudes $\{A_i\}^{II}$, $i = 1, 2, \cdots, N^{II}$.

In the next phase, the fields inside and outside the flaw are required to obey the continuity conditions on the surface of the object at a selected set of points. Consequently, this results in a matrix equation in which the amplitudes of the sources are the unknowns to be determined. Once the amplitudes are found, the analysis of the scattering problem is completed as all the fields may then be calculated in a straightforward manner without the need to carry out numerical integration. By choosing smooth field functions, they are likely to render the final solution accurate in the far zone and in the near zone as well. This method of computation is suitable to many problems and it involves matrix solutions rather than carrying out integrals.

METHOD OF SOLUTION

The cylindrical bubble shape imposes cylindrical coordinates (r, φ, x). The surface $r = a_0, \forall x\ (S)$ is identified with the interface between the interior of the flaw

and the adhesive, where a_0 is the cylinder radius. The various quantities related to the zone of the flaw are characterized by index 1 while the quantities denoted with the index 2 refer to the adhesive layer. Since the case considered is an air bubble, the wave component in the adhesive layer along the surface S, slides freely. The continuity of the displacement along the radius of the bubble provides the first boundary condition. The continuity of the stress along the radius as well as along the surface S, provides additional two boundary conditions. This leads to the boundary equations

$$\begin{aligned} u_r^s - u_r^t &= -u_r^i \qquad ; \qquad on \quad S \\ t_j^s - t_j^t &= -t_j^i \quad j = r, \varphi; \quad on \quad S. \end{aligned} \tag{4}$$

The subindex r represents continuity along the radius r, and the subindex φ represents continuity along the angle φ (surface S). Evidently, if sets of filamentary sources $\{A_i\}^I$ and $\{A_i\}^{II}$ could be found which strictly satisfy the continuity conditions (4), then (u^s, t^s) would be the exact field scattered by the cylinder and (u^t, t^t) would be the exact field inside the cylinder. We impose the continuity conditions (4) at N selected points on S. N is chosen equal to $N = N^I = N^{II}$, so the result is a $3N \times 3N$ matrix equation which can be subsequently solved for $\{A_i\}^I$ and $\{A_i\}^{II}$.

The acoustic potentials at an observation point due to a filament source radiation is given by the Hankel function of the second kind of zero order [4].

$$\begin{aligned} \phi &= AH_0^{(2)}(k_l r) \\ \psi &= BH_0^{(2)}(k_t r). \end{aligned} \tag{5}$$

Giving ϕ and ψ in cylindrical coordinates, leads to the following displacement and stress relations

$$\begin{array}{lcll} u_r & = & \frac{\partial \phi}{\partial r} & = -Ak_l H_1^{(2)}(k_l r) \\ u_\varphi & = & -\frac{\partial \psi}{\partial r} & = Bk_t H_1^{(2)}(k_t r) \\ t_{rr} & = & \lambda \nabla^2 \phi & = -A\lambda k_l^2 H_0^{(2)}(k_l r) \\ t_{r\varphi} & = & -\mu r \frac{\partial}{\partial r}\left(\frac{1}{r}\frac{\partial \psi}{\partial r}\right) & = -B\mu k_t^2 H_2^{(2)}(k_t r). \end{array} \tag{6}$$

The acoustic field (u^s, t^s) at an arbitrary observation point in region II is the sum of all the contributions due to the filament sources A^I radiating in this region

$$(u^s, t^s) = \sum_{i=1}^{N} (u_i^s, t_i^s) \tag{7}$$

where (u_i^s, t_i^s) are given by Eq. (6). The acoustic field (u^t, t^t) in region I is given by the sum of the filament radiations A^{II}, similarly to Eq. (7).

Evidently, the simulated fields must satisfy the boundary conditions over the surface S to some desired accuracy. The matrix equation to be solved as a consequence of imposing the boundary conditions is $[Z]A = E$. $[Z]$ is a square matrix because the number of match points had been chosen to be equal to the number of filament sources. If $[Z]$ is invertible, the exact solution is $A = [Z]^{-1}E$. The matrices

have the following form

$$[Z] = \begin{bmatrix} [Z_u^{A^I}] & [Z_u^{A^{II}}] & [Z_u^{B^I}] \\ [Z_{t_\varphi}^{A^I}] & [Z_{t_\varphi}^{A^{II}}] & [Z_{t_\varphi}^{B^I}] \\ [Z_{t_r}^{A^I}] & [Z_{t_r}^{A^{II}}] & [Z_{t_r}^{B^I}] \end{bmatrix}$$

$$A = \begin{bmatrix} [A^I] \\ [A^{II}] \\ [B^I] \end{bmatrix}$$

$$E = \begin{bmatrix} [u^i] \\ [t_\varphi^i] \\ [t_r^i] \end{bmatrix} . \tag{8}$$

In Eq. (8) $[Z_u^{A^I}]$ is an N by N matrix whose (i,j) element is the normal (to S) displacement at matching point i due to the normal displacement contribution from the filament j located inside the bubble. Similarly, $[Z_u^{A^{II}}]$ is an N by N matrix whose (i,j) element is the normal displacement at matching point i due to the normal displacement contribution from the filament j located outside the bubble. $[Z_u^{B^I}]$ is an N by N matrix whose (i,j) element is the shear displacement contribution to the normal component on S from the j filament inside the bubble. In a similar fashion we define the shear stress matrix $[Z_{t_\varphi}]$ and the normal stress $[Z_{t_r}]$. $[A^I]$ is an N column vector whose ith element is A_i^I. Similarly, $[A^{II}]$ is an N column vector whose ith element is A_i^{II} and the same for $[B^I]$. Finally, in E, $[u^i], [t_\varphi^i]$ and $[t_r^i]$ are N element column vectors whose ith element is the negative of the incident normal displacement, shear stress and normal stress respectively, on S.

NUMERICAL RESULTS

The materials investigated in this work consist of two type $Al2024^{TM}$ aluminum plates, bonded by $FM73^{TM}$ adhesive of $100\mu m$ thickness. The properties of $Al2024$ are $\rho_1 = 2.7gr/cm^3, V_l^1 = 6.32km/s, V_t^1 = 3.13km/s$ and for the adhesive $\rho_0 = 1.18gr/cm^3, V_l^1 = 2.25km/s, V_t^1 = 0.98km/s$. The thickness of the aluminum plates is 1.6 mm.

Let us compute the scattering function defined by

$$\sigma = \lim_{r\to\infty} 4\pi r^2 \frac{|P^s|^2}{|P^{inc}|^2}. \tag{9}$$

This is done by first solving for the complex amplitudes of the filaments for the case of an impinging guided wave and then calculating the total radiation. Results for the scattering problem of the first five modes in the acoustic waveguide from the air bubble are shown in Fig. 3. The cutoff frequency was chosen for each mode as the

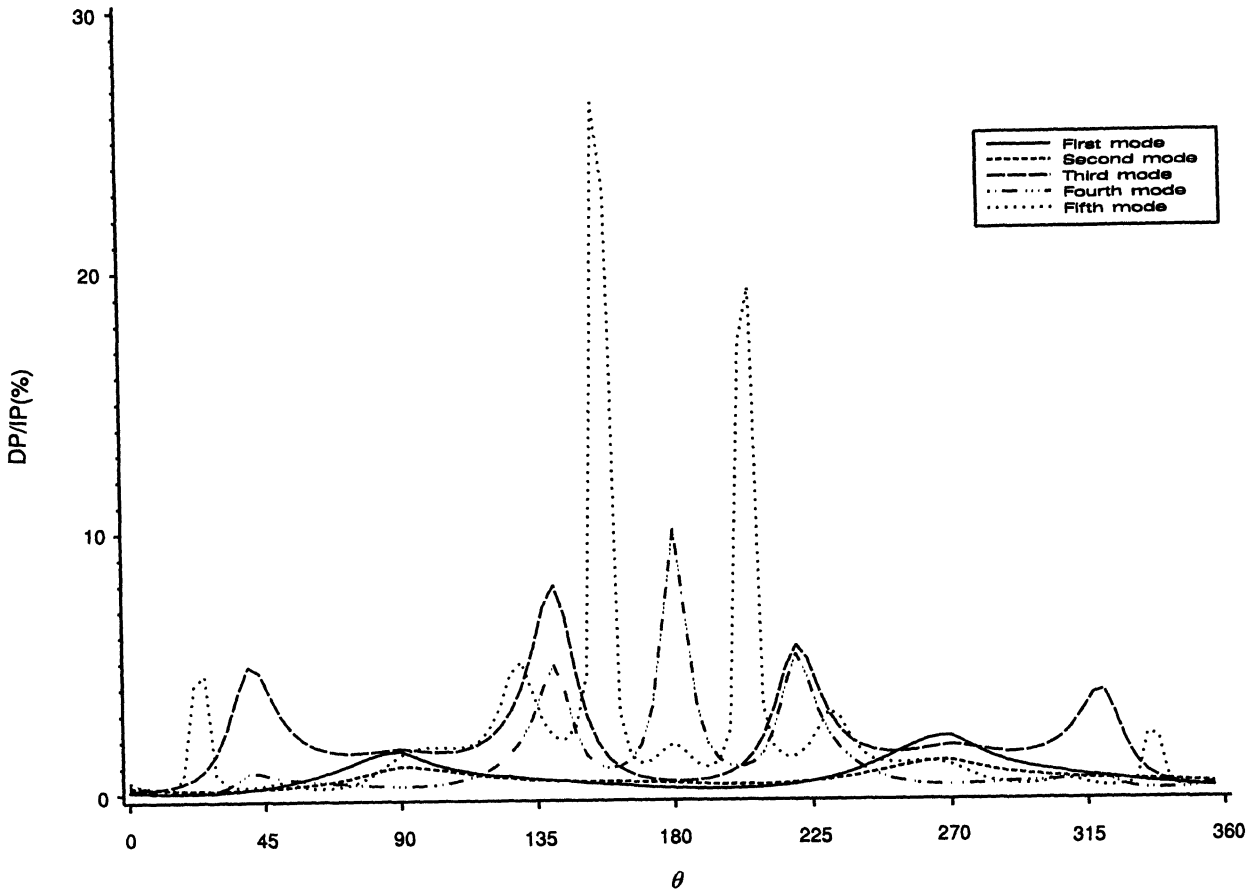

Figure 3: Scattered power normalized to the incident power as a function of the angle θ for the first five modes at the cutoff frequency.

frequency of inspection, thus as the impinging waveguide mode number increases, the wavelength to bubble radius decreases. The results indicate different behavior for the various modes used, as a function of the scattered angle θ. The highest modes tend to increase the scattered field while simultaneously the maximum angle of scattering is also moving. This can be explained by the fact that higher modes include more peaks within the waveguide region, therefore one can interpretate the incident of a high mode on the flaw as the incident of several lower modes. In most cases, the best inspection will be done using the first mode of the waveguide, for the location of the bubble. For the first mode, most of the scattered energy is located at two peaks, at the angle of $\theta = 90^{o}$ and 270^{o}. This means that it is possible to scan the laminate structure from above or at the bottom looking for diffraction fields from the flaws. By identifying the location of the scattered power, the position of the flaw is found.

CONCLUSIONS

It is evident from the previous discussion that the tool presented in this work can be used to analyze various parameters and their influence on the ultrasonic scattering characteristics by using this convenient method. This technique is applicable to scatterers of smooth, but otherwise arbitrary, cross section. The present study can serve as a basis for the detections of small defects in plate structures. For the air bubble, it is possible to measure its dimension and location in the laminant. This can also be done by using the standard backscattering cross-section but this method excludes the use of numerical integration. It is also possible to expand the calculations to additional flaws. The method presented here can be generalized for any problem which involves scattering as long as the characteristic dimensions of the defect are bigger than those of the wavelength. Otherwise, approximation of the problem can be easily reduced to the Minkowski problem: restoration of convex defect shape over the given Gauss surface curvature.

REFERENCES

1. White, R.M. Elastic wave scattering at a cylindrical discontinuity in solid *J. Acoust. Soc. Am.*, Vol. 30, p. 771 (1958).
2. Singher, L., Segal, Y., Segal, E. and Shamir, J. Considerations in bond strength evaluation by ultrasonic guided waves *J. Acoust. Soc. Am.*, Vol. 96, pp. 2497-2505 (1994).
3. Truell, R., Elbaum, C. and Chick, B.B., *Ultrasonic methods in solid state physics*, Academic Press, p. 9 (1969).
4. Harrington, R.F. *Time-harmonic electromagnetic fields*, McGraw-Hill Book Company, p. 224 (1961).